

Research Article

Adaptively Receding Galerkin Optimal Control for a Nonlinear Boiler-Turbine Unit

Gang Zhao,¹ Zhi-gang Su ,¹ Jun Zhan,¹ Hongxia Zhu,² and Ming Zhao³

¹School of Energy and Environment, Southeast University, Nanjing, Jiangsu 210096, China

²School of Energy and Power Engineering, Nanjing Institute of Technology, Nanjing, China

³Research Institute of Yunnan Power Grid Co. Ltd., Kunming, Yunnan, China

Correspondence should be addressed to Zhi-gang Su; zhigangsu@seu.edu.cn

Received 14 April 2018; Accepted 3 June 2018; Published 1 August 2018

Academic Editor: Jing Na

Copyright © 2018 Gang Zhao et al. This is an open access article distributed under the Creative Commons Attribution License, which permits unrestricted use, distribution, and reproduction in any medium, provided the original work is properly cited.

The boiler-turbine unit is really a complex system in thermal power engineering due to its large-scale nonlinearity, unmeasured state, unknown disturbances, and constraints imposed on both controls and outputs. To design a controller with appropriate performance in above synthetical cases, this paper intends to propose an adaptively receding Galerkin optimal controller design method, in which, the mathematical dynamics of unit can be directly used as a predictive model without any linearization, and the unmeasured state in the predictive model is adaptively estimated using a predesigned state observer. With the help of a mathematical predictive model, optimal control law is then obtained based on a Galerkin optimization algorithm. Due to the application of the useful information measured at every sampling time instant, the proposed method can deal with the tracking problem with constraints rather than the stabilization problem that can be only done by the traditional Galerkin optimal control. Furthermore, it can also be easily extended to estimate and thus eliminate constant disturbances in an output channel using an independent model strategy. Some simulations suggest that satisfactory tracking performance can be achieved even when the unit experiences wide-range load change.

1. Introduction

The boiler-turbine unit plays a critical role in a thermal power plant. Due to its genuine nonlinearity, serious couplings among state variables, and physical constraints, it is difficult to design a controller with appropriate transient performance for the boiler-turbine unit [1]. In particular, some key unmeasured state variables as well as unknown disturbances bring much more difficulties in controlling the boiler-turbine unit.

Conventionally, the boiler-turbine unit was usually operated in a local load range. In this way, the proportional-integral-differential (PID) controller can achieve acceptable performance [2]. However, the unit should be run now in a large-scale load range, which leads the unit's dynamics to be inherently nonlinear [3]. In this case, it is challenging to design a PID controller with appropriate performance,

especially when some physical constraints are required for a safe and correct functioning of the unit. To achieve better performance, recent years witness a surge of interests on designing an advanced controller for the popular oil-fired drum-type boiler-turbine unit [1], for example, see [3–19] and the literature therein. As for the boiler-turbine unit, it is interesting and imperative to derive new control strategy that can maximize or minimize a specified control performance index while honoring the constraints imposed on the unit. Until now, several optimal controllers such as model predictive control have been investigated and achieved better performances for the unit [4, 10–13, 15, 16]. Nevertheless, most of these controllers were designed on the basis of either the black-box nonlinear model identified from running data of the unit or linear models obtained by linearizing the unit's mathematical model. More attentions recently have been paid to optimal controller design, for example,

see [20]. How to design an optimal controller directly based on the unit's mathematical model with appropriate tracking performance is still open.

When designing an optimal controller for either the unit or other nonlinear systems, it has been well recognized as an extremely challenging problem to analytically solve a state- and control-constrained nonlinear optimal control problem in particular in real-time applications. As a matter of fact, due to the genuine large-scale nonlinearity of the unit, it is widely considered to be difficult to solve an optimal controller for the unit even in nonreal time. The main difficulty arises in seeking a closed-form solution to the Hamilton-Jacobi equation or in solving the canonical Hamiltonian equations resulting from an application of the minimum principle [21]. Alternatively, a Galerkin pseudospectral method [22, 23] is one of the most efficient computational approaches, intending to solve the optimal state and control sequences through transforming the state- and control-constrained nonlinear optimal control problems into a nonlinear programming problem [18, 24]. There are some obstacles on the path to design a Galerkin optimal controller to make the unit track large-scale load demand/reference. Firstly, either the Galerkin method or other pseudospectral methods usually pay much more attentions to the stabilization problem rather than the tracking problem. To solve the tracking problem, the Galerkin method should be receding or rolling in some sense by making use of the useful information measured at every sampling time instant. Secondly, to make use of information at every sampling time instant, it requires all state variables to be measurable. It will be seen that the key unmeasured state *fluid density* in the drum of the unit is unmeasurable. Finally, some unknown (constant) disturbances in the output channels bring much more difficulties. How to compensate uncertainties/disturbances so as to enhance control performance can be referred, for example, to [25–27].

Motivated by above statements, this paper aims to propose an adaptively receding Galerkin optimal control method for an oil-fired drum-type boiler-turbine unit with some unmeasured states as well as some unknown constant disturbances in the output channels. More precisely, a state observer is first designed to adaptively estimate the key unmeasured state so as to make the information available at every sampling time instant; then, a receding Galerkin optimal controller is constructed by sufficiently taking into account information observed at each sampling time, through borrowing the basic idea from the model predictive control method; after this, an independent model strategy is embedded into the receding Galerkin controller structure to estimate and thus eliminate the constant disturbances in the output channels. Evidently, the main contributions of this paper are in twofold: an adaptively receding Galerkin optimal control strategy with estimations of unmeasured state and unknown constant output disturbances and its application for a boiler-turbine unit.

The rest of the paper is organized as follows. Section 3 briefly recalls the Galerkin method. In Section 5, the receding Galerkin optimal control strategy is proposed after introducing the boiler-turbine unit, including the state observer and

the independent model strategy. Simulation results are presented in Section 4. The last section concludes this paper.

2. Galerkin Method

The main purpose of the optimal control is to solve out the admissible control sequences minimizing a cost function based on the mathematical model of an object. The mathematical description of an optimal control problem can be described as follows: determine the state-control function pair, $t \rightarrow (x, u) \in R^{N_x} \times R^{N_u}$ minimizing the following cost functional (or called a performance index)

$$J = \int_{t_0}^{t_f} F(x(t), u(t)) dt + E(x(t_f)), \quad (1)$$

subject to the dynamics

$$\dot{x}(t) = f(x(t), u(t)), \quad (2)$$

initial conditions

$$x(t_0) = x_0, \quad (3)$$

endpoint conditions

$$e(x(t_f)) = 0, \quad (4)$$

and path constraints

$$h(x(t), u(t)) \leq 0, \quad (5)$$

where the running (or Lagrange) cost $F : R^{N_x} \times R^{N_u} \rightarrow R$, the endpoint (or Mayer) cost $E : R^{N_x} \times R^{N_x} \rightarrow R$, $f : R^{N_x} \times R^{N_u} \rightarrow R^{N_x}$, $e : R^{N_x} \times R^{N_u} \rightarrow R^{N_e}$, and $h : R^{N_x} \times R^{N_u} \rightarrow R^{N_h}$ are all Lipschitz continuous.

A Galerkin method transforms the above problem into a nonlinear programming problem through the following four steps: approximating state and control variables, discretizing the system dynamics, integrating the cost function, and discretizing other constraints.

To realize approximation or discretization, it needs to introduce the concept of the *node*. By converting the real-time domain $t \in [t_0, t_f]$ into a closed interval $\tau \in [-1, 1]$ according to

$$\tau = \frac{2t - (t_f + t_0)}{t_f - t_0}, \quad (6)$$

a series of Legendre-Gauss-Lobatto (LGL) nodes can be calculated as the roots of

$$\xi(\tau) = (1 - \tau^2) \dot{L}_N(\tau), \quad (7)$$

where $L_N(\tau)$ is the N th order Legendre polynomial defined by $L_N(\tau) = ((-1)^N / 2^N N!) (d^N / d\tau^N) (1 - \tau)^N$. Obviously, there are $(N + 1)$ LGL nodes in τ -space such that

$$\{\tau_i\}_{i=0}^N \quad (\tau_0 = -1 < \tau_1 < \tau_2 < \dots < \tau_N = 1), \quad (8)$$

which correspond to $t^{(N_i)}_{(i=0)} = \{t_0 = t^{(N_0)} < t^{(N_1)} < \dots < t^{(N_N)} = t_f\}$ in the real-time domain.

In this way, one has $x(t) = x(\tau)$, $u(t) = u(\tau)$, or more specifically $x^{N_i} = x(t^{N_i}) = x(\tau_i)$, $u^{N_i} = u(t^{N_i}) = u(\tau_i)$, $i = 0, 1, \dots, N$. With the help of LGL nodes, a Galerkin method approximates the state and control by the N th order Lagrange interpolation polynomial defined on LGL nodes as follows:

$$\begin{aligned} x(\tau) &\approx \sum_{j=0}^N \phi_j^N(\tau) \cdot x^{N_j}, \\ u(\tau) &\approx \sum_{j=0}^N \phi_j^N(\tau) \cdot u^{N_j}, \end{aligned} \quad (9)$$

where $\phi_j^N(\tau)$ is the N th order Lagrange interpolation basis function defined by $\phi_j^N(\tau) = \prod_{i=0, i \neq j}^N ((\tau - \tau_i) / (\tau_j - \tau_i))$.

Using (9), the differential equation (2) can be approximated using the following integral formulation:

$$\int_{-1}^1 \psi_i(\tau) \left(\dot{x}(\tau) - \frac{t_f - t_0}{2} f(x(\tau), u(\tau)) \right) d\tau = 0, \quad (10)$$

with test functions $\psi_i(\tau)$. When defining test function as equal to the basis function $\phi_j^N(\tau)$, (10) can be rewritten as

$$\sum_{j=0}^N \int_{-1}^1 \phi_i(\tau)^N \dot{\phi}_j^N(\tau) d\tau \cdot x^{N_j} - \frac{t_f - t_0}{2} \int_{-1}^1 f(x(\tau), u(\tau)) d\tau = 0. \quad (11)$$

For simplicity, define $D_{ij} = \int_{-1}^1 \phi_i(\tau)^N \dot{\phi}_j^N(\tau) d\tau$ and $\Delta_i = ((t_f - t_0)/2) \int_{-1}^1 f(x(\tau), u(\tau)) d\tau$. The following two approximate equalities can be induced:

$$\begin{aligned} D_{ij} &\approx \sum_{k=0}^N \phi_i(\tau_k)^N \dot{\phi}_j^N(\tau_k) w_k \approx \dot{\phi}_j^N(\tau_i) w_i = \mathbf{A}_{ij} w_i, \\ \Delta_i &\approx \frac{t_f - t_0}{2} f(x(\tau_i), u(\tau_i)) w_i, \end{aligned} \quad (12)$$

where \mathbf{A}_{ij} is the Legendre differentiation matrix calculated by $\mathbf{A}_{ij} = (L_N(\tau_i) / L_N(\tau_j)) (1 / (\tau_i - \tau_j))$ for $i \neq j$, $\mathbf{A}_{ij} = (-N(N+1)/4)$ for $i = j = 0$, and $\mathbf{A}_{ij} = (N(N+1)/4)$ for $i = j = N$, otherwise 0, $i = j \in [1, \dots, N-1]$, and w_i s are the quadrature weights, and the LGL version of quadrature weights can be calculated as

$$w_i = \frac{2}{N(N+1)[L_N(\tau_i)]}, \quad i = 0, 1, \dots, N. \quad (13)$$

With the help of D_{ij} and Δ_i , (11) can thus be finally simplified as

$$\sum_{j=0}^N D_{ij} \cdot x^{N_j} - \Delta_i = 0, \quad i = 0, 1, \dots, N. \quad (14)$$

In a relatively easy way, the cost function (1) can then be approximated according to the Gauss-Lobatto integration rule as follows:

$$\begin{aligned} J &= \int_{t_0}^{t_f} F(x(t), u(t)) dt + E(x(t_f)) \\ &= \frac{t_f - t_0}{2} \sum_{j=0}^N F(x^{N_j}, u^{N_j}) w_j + E(x^{N_N}). \end{aligned} \quad (15)$$

Finally, together with the following approximations

$$x^{N_0} = x_0, e(x^{N_N}) = 0, h(x^{N_i}, u^{N_i}) \leq 0, \quad i = 0, 1, \dots, N, \quad (16)$$

the Galerkin method transforms the continuous optimal control problems (2), (3), (4), and (5) into the following discrete nonlinear programming problem:

$$\begin{aligned} \min_{x^{N_j}, u^{N_j}} \quad & J = \frac{t_f - t_0}{2} \sum_{j=0}^N F(x^{N_j}, u^{N_j}) w_j + E(x^{N_N}) \\ \text{s.t.} \quad & \left\| \sum_{j=0}^N D_{ij} \cdot x^{N_j} - \Delta_i \right\|_{\infty} \leq \delta^N, \\ & \|x^{N_0} - x_0\|_{\infty} \leq \delta^N, \\ & \|(e^{N_N})\|_{\infty} \leq \delta^N, \\ & h(x^{N_i}, u^{N_i}) \leq \delta^N, \quad i, j = 0, 1, \dots, N, \end{aligned} \quad (17)$$

where δ^N is a constant tolerance used to guarantee feasibility of the nonlinear programming problem [21].

To solve a discrete nonlinear programming problem (17), a nonlinear programming solver such as SNOPT and IPOPT is usually used [21].

3. Main Results

3.1. Problem Formulations and Adaptively Receding Galerkin Strategy. This paper considers a 160 MW oil-fired drum-type boiler-turbine unit [1], whose flow diagram is summarized in Figure 1. The mathematical model of this unit has been established in a form of

$$\dot{x}_1 = f_1(x, u) = -0.0018u_2x_1^{1.125} + 0.9u_1 - 0.15u_3, \quad (18)$$

$$\dot{x}_2 = f_2(x, u) = (0.073u_2 - 0.16)x_1^{1.125} - x_2, \quad (19)$$

$$\dot{x}_3 = f_3(x, u) = \frac{(141u_3 - (1.1u_2 - 0.19)x_1)}{85}, \quad (20)$$

$$y_1 = x_1, \quad (21)$$

$$y_2 = x_2, \quad (22)$$

$$y_3 = h(x, u) = 0.05 \left(0.13073x_3 + 100\alpha_{cs} + \left(\frac{q_e}{9 - 67.975} \right) \right). \quad (23)$$

where x_1 is drum pressure (kg/cm²); x_2 is electrical output (MW); x_3 is fluid density in the drum (kg/cm³); outputs y_1 , y_2 , and y_3 are, respectively, the drum steam pressure, electrical output, and drum water level; u_1 , u_2 , and u_3 are, respectively, the normalized fuel flow rate, control

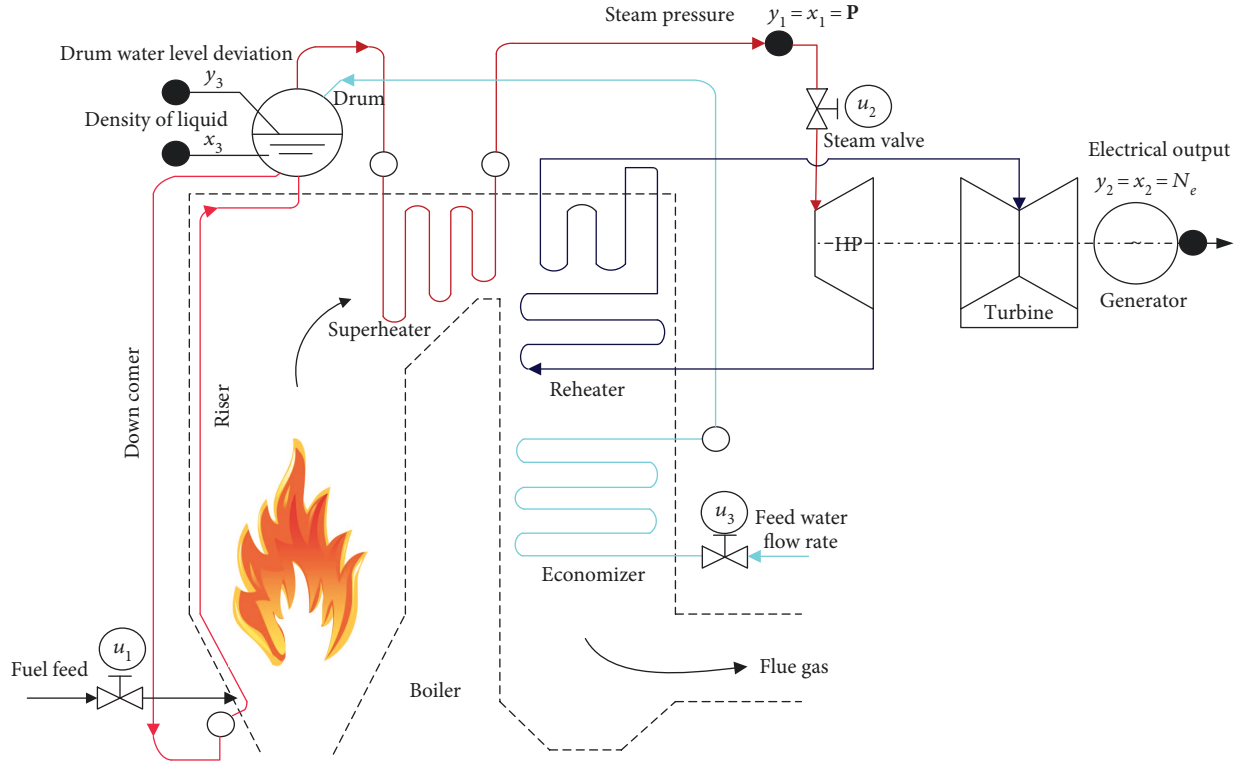


FIGURE 1: Structure of a 160 MW boiler-turbine unit in a thermal power plant.

valve position, and feedwater flow rate; and the coefficient α_{cs} and evaporation rate of steam q_e (kg/s) are defined, respectively, as

$$\alpha_{cs} = \frac{(1 - 0.001538x_3)(0.8x_1 - 25.6)}{x_3(1.0394 - 0.0012304x_1)}, \quad (24)$$

$$q_e = (0.854u_2 - 0.147)x_1 + 45.59u_1 - 2.514u_3 - 2.096. \quad (25)$$

For safety consideration, models (18), (19), (20), (21), (22), and (23) should satisfy the following constraints [1, 5]:

$$\begin{aligned} u_i' &\in [0, 1], \\ |\dot{u}_1| &\leq 0.007, \\ |\dot{u}_2| &\leq 0.02, \\ |\dot{u}_3| &\leq 0.05, \end{aligned} \quad (26)$$

$$\begin{aligned} y_1 &\in [70, 150], \\ y_2 &\in [10, 190], \\ y_3 &\in [-0.1, 0.1]. \end{aligned}$$

Remark 1. Models (18), (19), (20), (21), (22), and (23) indicate that the unit's behaviors are genuinely nonlinear and state variables are seriously coupled. In particular, the state x_3 is unmeasurable. Furthermore, as will be seen, (constant) output disturbances will be considered. All these facts put some obstacles on the path to design a receding Galerkin optimal controller for the unit straightforwardly.

Galerkin optimal control for boiler-turbine unit: define $v = [v_1, v_2, v_3]'$ such that $v_1 = \dot{u}_1/c_1$, $v_2 = \dot{u}_2/c_2$, and $v_3 = \dot{u}_3/c_3$ with expansion coefficients c_i 's, the optimal control problem for the unit can be formulated as (utilizing (18), (19), (20), (21), (22), and (23))

$$\begin{aligned} \min_{x,v} \quad & J_{BT} = \int_{t_0}^{t_f} [(y - yr)'P(y - yr) + v'Qv] dt \\ \text{s.t.} \quad & \dot{u}_1 = c_1 v_1, \\ & \dot{u}_2 = c_2 v_2, \\ & \dot{u}_3 = c_3 v_3, \end{aligned} \quad (27)$$

where the outputs $y = [y_1, y_2, y_3]'$, output references $yr = [y_{1r}, y_{2r}, y_{3r}]'$, and $u = [u_1, u_2, u_3]'$; \dot{u} is the controllers' derivatives; P and Q are positive definite weight matrices. By introducing $c = [c_1, c_2, c_3]'$, the states and change of controls can now satisfy

$$\begin{aligned} 70 &\leq x_1 \leq 150, \\ 10 &\leq x_2 \leq 190, \\ 0 &\leq u_1, u_2, u_3 \leq 1, \\ |v_1| &\leq \frac{0.007}{c_1}, \\ |v_2| &\leq \frac{0.02}{c_2}, \\ |v_3| &\leq \frac{0.05}{c_3}, \end{aligned} \quad (28)$$

and the path constraints $h(x, u) - 0.1 \leq 0$ and $-h(x, u) - 0.1 \leq 0$.

It is evident that the current Galerkin method interpreted in Section 3 is only feasible for the stabilization problem rather than the tracking problem. To deal with the tracking problem, it should take into account the useful information measured at each sampling time instant, including the information of states, outputs, and references. To solve this problem, a receding version of Galerkin optimal control strategy is proposed straightforward by borrowing the basic idea from model predictive control as below.

- (i) At current time instant t_k , let the current state $x(t_k)$ and control $u(t_k)$ be the initial conditions, that is, $x_{0,k} = x(t_k)$, $u_{0,k} = u(t_k)$; then, obtain the optimal discrete state and control sequences $\{x^{N_j,k}\}$ and $\{u^{N_j,k}\}$ by minimizing J_{BT} through the Galerkin method over the prediction horizon $[t_0, t_f] = [t_k, t_k + \Delta T]$, where ΔT is the length of horizon. More precisely, we have

$$\begin{aligned} \min_{\{x^{N_j,k}, u^{N_j,k}, v^{N_j,k}\}} J_{BT} &= \frac{\Delta T}{2} \sum_{j=0}^N \left[\left(y^{N_j,k} - y_r^{N_j,k} \right)' \mathbf{P} \right. \\ &\quad \cdot \left(y^{N_j,k} - y_r^{N_j,k} \right) \\ &\quad \left. + v^{N_j,k'} \mathbf{Q} v^{N_j,k} \right] w_j \\ \text{s.t.} \quad &\left\| \sum_{j=0}^N D_{ij} \begin{bmatrix} x^{N_j,k} \\ u^{N_j,k} \end{bmatrix} - \Delta_i \right\|_{\infty} \leq \delta^N, \\ &\left\| x^{N_{0,k}} - x_{0,k} \right\|_{\infty} \leq \delta^N, \\ &\left\| u^{N_{0,k}} - u_{0,k} \right\|_{\infty} \leq \delta^N, \\ &h(x^{N_j,k}, u^{N_j,k}) - 0.1 \leq \delta^N, \\ &-h(x^{N_j,k}, u^{N_j,k}) - 0.1 \leq \delta^N, \quad i, j = 0, 1, \dots, N, \end{aligned} \quad (29)$$

with $y^{N_j,k} = [x_1^{N_j,k}, x_2^{N_j,k}, h(x^{N_j,k}, u^{N_j,k})]'$ and $\Delta_i = [f_1(\cdot), f_2(\cdot), f_3(\cdot), c_1 v_1^{N_j,k}, c_2 v_2^{N_j,k}, c_3 v_3^{N_j,k}]'$. Note that the superscript k in variables such as $x^{N_j,k}$ and $u^{N_j,k}$ is just used to distinguish optimal solutions at different sampling time instants.

- (ii) Apply the optimal control law $u^{N_{1,k}}$ on the unit and repeat the above operations in step (i) at the coming time instant t_{k+1} .

3.2. Receding Galerkin Optimal Control with a State Observer.

In order to implement the receding Galerkin optimal controller, all the states should be known in advance. However, the state variable x_3 , that is, the fluid density in the drum,

cannot be measured online. Therefore, we design a state observer to estimate the unmeasured state x_3 as follows.

Proposition 1. *The following observer can render the unmeasured state in the unit (18), (19), (20), (21), (22), and (23) asymptotically to its true value:*

$$\dot{\hat{x}}_3 = \frac{(141u_3 - (1.1u_2 - 0.19)x_1)}{85 + l(y_3 - \hat{y}_3)}, \quad (30)$$

where $\hat{y}_3 = 0.05(0.13073\hat{x}_3 + 100\hat{\alpha}_{cs} + (q_e/9 - 67.975))$ with $\hat{\alpha}_{cs} = (1 - 0.001538\hat{x}_3)(0.8x_1 - 25.6)/\hat{x}_3(1.0394 - 0.0012304x_1)$, and constant l is observer gain.

Proof. Define the error $e = x_3 - \hat{x}_3$, whose derivative results in

$$\begin{aligned} \dot{e} &= \dot{x}_3 - \dot{\hat{x}}_3 = -l(y_3 - \hat{y}_3) = -l \cdot 0.05(0.13073(x_3 - \hat{x}_3) \\ &\quad + 100(\alpha_{cs} - \hat{\alpha}_{cs})) = -l \cdot 0.05 \left(0.13073 - \beta(x_1) \frac{100}{x_3 \hat{x}_3} \right) e, \end{aligned} \quad (31)$$

with $\beta(x_1) = (0.8x_1 - 25.6)/(1.0394 - 0.0012304x_1)$.

Note that $x_1 \in [70, 150]$, then one can conclude $\beta(x_1) \leq 110.43$ (when $x_1 = 150$, $\beta(x_1)$ takes the maximum value), which together with $x_3 \geq 299.6$ leads to

$$\beta(x_1) \frac{100}{x_3 \hat{x}_3} \leq 110.43 \cdot \frac{100}{x_3 \hat{x}_3} \leq 110.43 \cdot \frac{100}{299.6 \hat{x}_3} \leq \frac{36.86}{\hat{x}_3}. \quad (32)$$

If $\hat{x}_3 > 299.6$, like the real range of the state x_3 , one has

$$0.13073 - \beta(x_1) \frac{100}{x_3 \hat{x}_3} > 0.13073 - \frac{36.86}{\hat{x}_3} > 0. \quad (33)$$

It means that as long as $\hat{x}_3(0) > 299.6$, we can achieve $\dot{e} = -\bar{l}e$ with a positive coefficient \bar{l} . In fact, it is reasonable to preset any initial value for state \hat{x}_3 in its practical range. To this end, the estimated value of state \hat{x}_3 can asymptotically converge to its true value.

Remark 2. To show the performance of the above state observer, a simple simulation is conducted here with $\hat{x}_3(0) = 440 \text{ kg/cm}^3$ and $x_1(0) = 100 \text{ kg/cm}^2$ under constant control inputs $u = [0.2, 0.6, 0.3]'$. The performance is shown in Figure 2, where the true trajectory of x_3 is obtained according to (20) with initial condition $x_3(0) = 449.5 \text{ kg/cm}^3$ and other conditions as the same as the observer. It suggests that the larger the constant l is, the observer approaches to the true trajectory faster.

With the help of Proposition 1, the estimated state $\hat{x}_3(k)$ at the k th sampling time instant will be taken as the initial condition for real $x_3(k)$ to implement the receding Galerkin method. Figure 3 presents the block diagram of the receding Galerkin optimal control strategy with the state observer for the unit.

3.3. Receding Galerkin Optimal Control with an Independent Model. There are always different versions of disturbances in practice for the unit. By considering the fact that the unit is

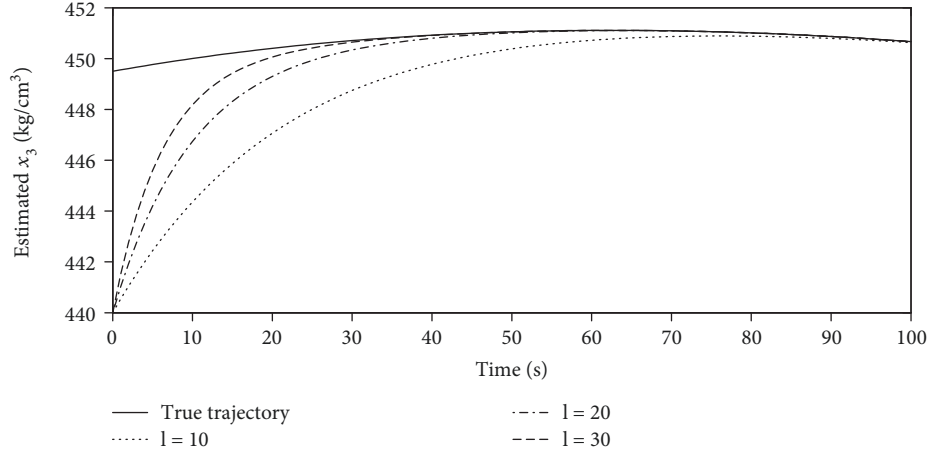
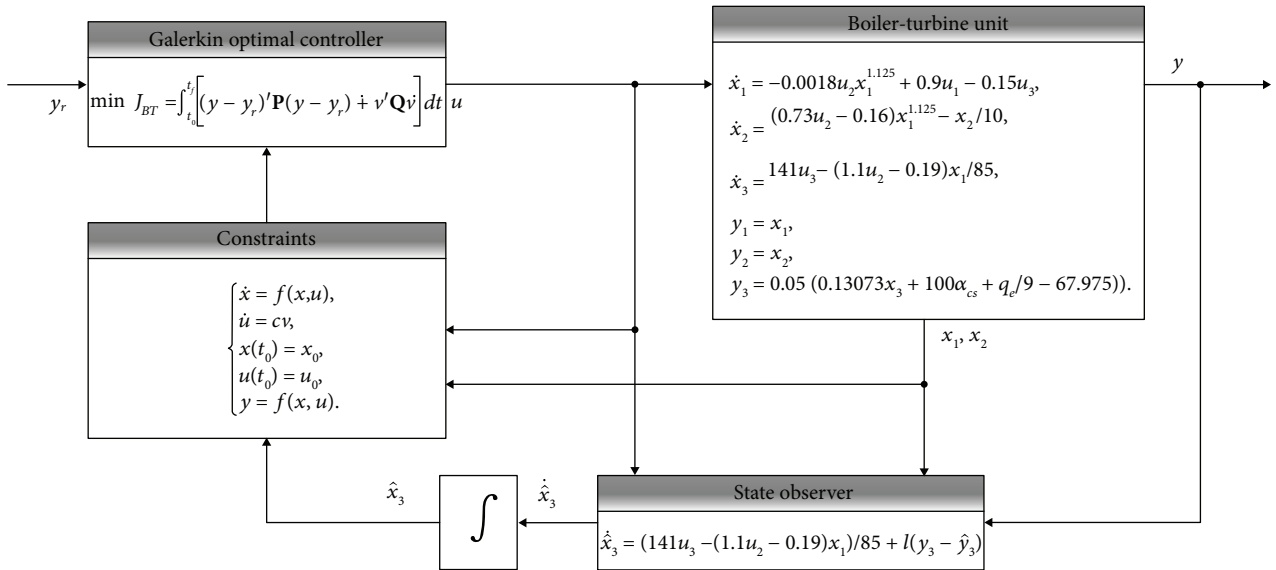
FIGURE 2: Performance of state observer for x_3 .

FIGURE 3: Block diagram used to implement the receding Galerkin method with the state observer.

usually slowly time-varying, we just consider constant disturbance $d = [d_1, d_2, d_3]'$ in the output channels in this paper. More precisely, we hold (18), (19), (20), and the following

$$\begin{aligned} y_1 &= x_1 + d_1, \\ y_2 &= x_2 + d_2, \\ y_3 &= 0.05 \left(0.13073x_3 + 100\alpha_{cs} + \left(\frac{q_e}{9 - 67.975} \right) \right) + d_3. \end{aligned} \quad (34)$$

In order to estimate the constant output disturbances, an independent model strategy can be introduced into the receding Galerkin optimal control strategy with the state observer, as shown in Figure 4.

It can be seen from Figure 4 that the constant output disturbance d can be estimated according to

$$\hat{d} = y_p - y_m, \quad (35)$$

where $y_p = y + d$ is the practical output and y_m is the output of an independent model. Here, the independent model is simply defined as the same as models (18), (19), (20), (21), (22), and (23). To this end, the estimated disturbances \hat{d} are fed back instead of d in (33) to implement the receding Galerkin method.

Remark 3. The existence of constant output disturbance d does not affect the estimation of unmeasured state x_3 . This is because the error $e_d = d - \hat{d}$ in $\dot{e} = -\bar{l}(e + e_d)$ will disappear at the coming sampling time instant once the constant output disturbance d appears. In practice, the mathematic model of the unit is not accurate, which means (34) cannot estimate d perfectly. In this case, the error e_d cannot be zero but be bounded. In this way, the estimate error e will just approach zero.

Remark 4. For either the unit (18), (19), (20), (21), (22), and (23) or the one with constant output disturbances like (18),

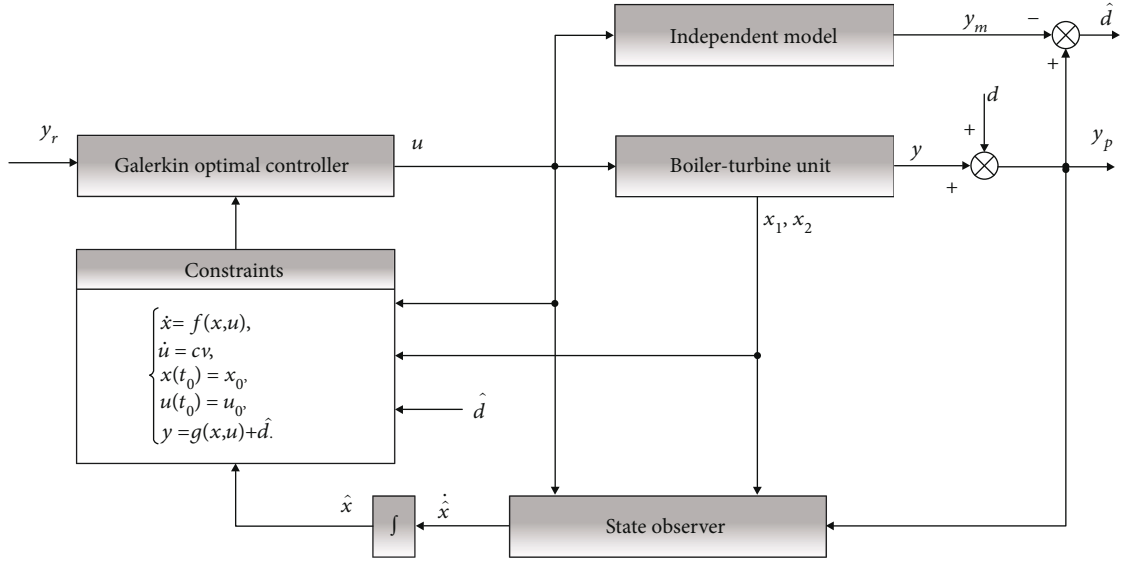


FIGURE 4: Block diagram used to implement the receding Galerkin method with the independent model.

(19), (20), (21), (22), (23), (24), (25), (27), (28), (29), (30), (31), (32), and (33), the solutions of problem (27) do in fact exist by selecting appropriate feasibility tolerance δ^N and the order of approximation N , as remarked in [21, 23]. Precise bounds for δ^N can be found experimentally using a recursive refinement process through increasing the order of approximation N until all the constraints in a nonlinear programming problem like (27) are satisfied.

4. Simulation

In this section, some simulations are conducted to validate the performance of receding Galerkin optimal control strategy for the oil-fired drum-type boiler-turbine unit.

To implement the receding Galerkin optimal control strategy, a nonlinear programming solver SNOPT is adopted and some controller parameters should be preset in advance such as $l, N, \delta^N, c_i^l s, t_0, t_f, \mathbf{P}$, and \mathbf{Q} . Suppose the sampling time for the unit is T_s . Due to the fact that only the second component in the optimal control sequence should be applied on the unit, the first two approximate time points in t -time domain should satisfy $t^{N_1} - t^{N_0} = T_s$. Therefore, with a given node number N , according to (6), we can determine the terminal time t_f as

$$t_f = t_0 + 2 \frac{t^{N_1} - t^{N_0}}{\tau_1 - \tau_0} = t_0 + \frac{2T_s}{\tau_1 + 1}, \quad (36)$$

where $t_0 = t_k$ at the k th sampling time instant, and τ_1 can be calculated by (7). During our simulations, we suggest $T_s = 1$ s.

We choose $l = 30$, $\delta^N = 10^{-5}$ in what follows and will discuss the influences of $N, c_i^l s, \mathbf{P}$, and \mathbf{Q} on the closed-loop system in Section 4.1. In Section 4.2, we continuously validate the controller performance through several study cases.

4.1. Influences of Controller Parameters. For simplicity in this section, the states, outputs, and control inputs are initialized for all study cases as follows: $x(0) = [100, 50, 449.5]^T$, $y_3(0) = 0$, $\hat{x}_3(0) = 445$, and $u(0) = [0.271, 0.604, 0.337]^T$. The outputs $y_i^l s$ aim to track constant references $y_{1r} = 110, y_{2r} = 55$, and $y_{3r} = 0$, respectively.

Firstly, we focus on the influence of the node number N on the performance of the closed-loop system by considering $N = \{10, 20, 30\}$. Given $c_i^l s = 0.001, i = 1, 2, 3, \mathbf{P} = \text{diag}\{1, 1, 2000\}, \mathbf{Q} = \text{diag}\{2, 1, 2\}$, where $\text{diag}\{\cdot\}$ indicates a diagonal matrix. The simulation results are shown in Figure 5, from which we can see that too small value of N (e.g., $N = 10$ here) usually leads to unappropriate performance and that a larger value of N leads to faster responses as well as control inputs. While N raises up to a certain limit, the responses and control inputs will change slightly but with an increasing heavy burden of computation. In what follows, we prefer to select $N = 20$. Correspondingly, the length of prediction horizon can be calculated as $\Delta T = t_f - t_0 = 103.63$ s.

With fixing $N = 20, \mathbf{P} = \text{diag}\{1, 1, 2000\}$, and $\mathbf{Q} = \text{diag}\{2, 1, 2\}$, we can now test the influence of expansion coefficients $c_i^l s$ on the performance of the closed-loop system. Here, we just consider identical $c_i^l s$ by taking values in $\{0.1, 0.01, 0.001\}$ for all $i = 1, 2, 3$. Simulation results are illustrated in Figure 6, which indicates that larger $c_i^l s$ usually result in faster responses with drastic changes of control inputs. To guarantee the constraints imposed on the changes of controls, we prefer smaller $c_i^l s$, that is, we suggest $c_i^l s = 0.001$ for all $i = 1, 2, 3$.

Besides N and $c_i^l s$, matrixes \mathbf{P} and \mathbf{Q} in the performance index J_{BT} also play a critical role. To see an insight, by fixing $N = 20$ and $c_i^l s = 0.001$, we consider the following three cases: (1) $\mathbf{P} = \text{diag}\{1, 1, 2000\}, \mathbf{Q} = \text{diag}\{2, 1, 2\}$, (2)

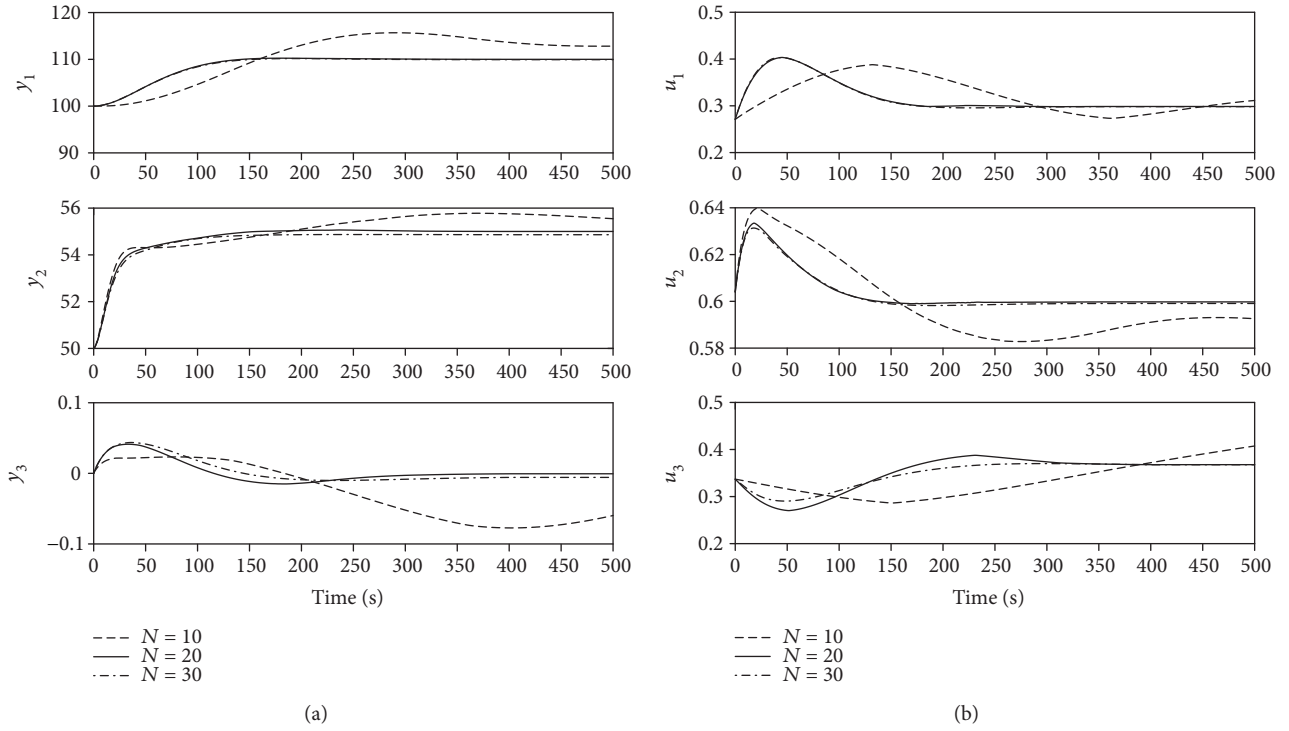


FIGURE 5: Outputs and controls of the unit when taking different number N of nodes.

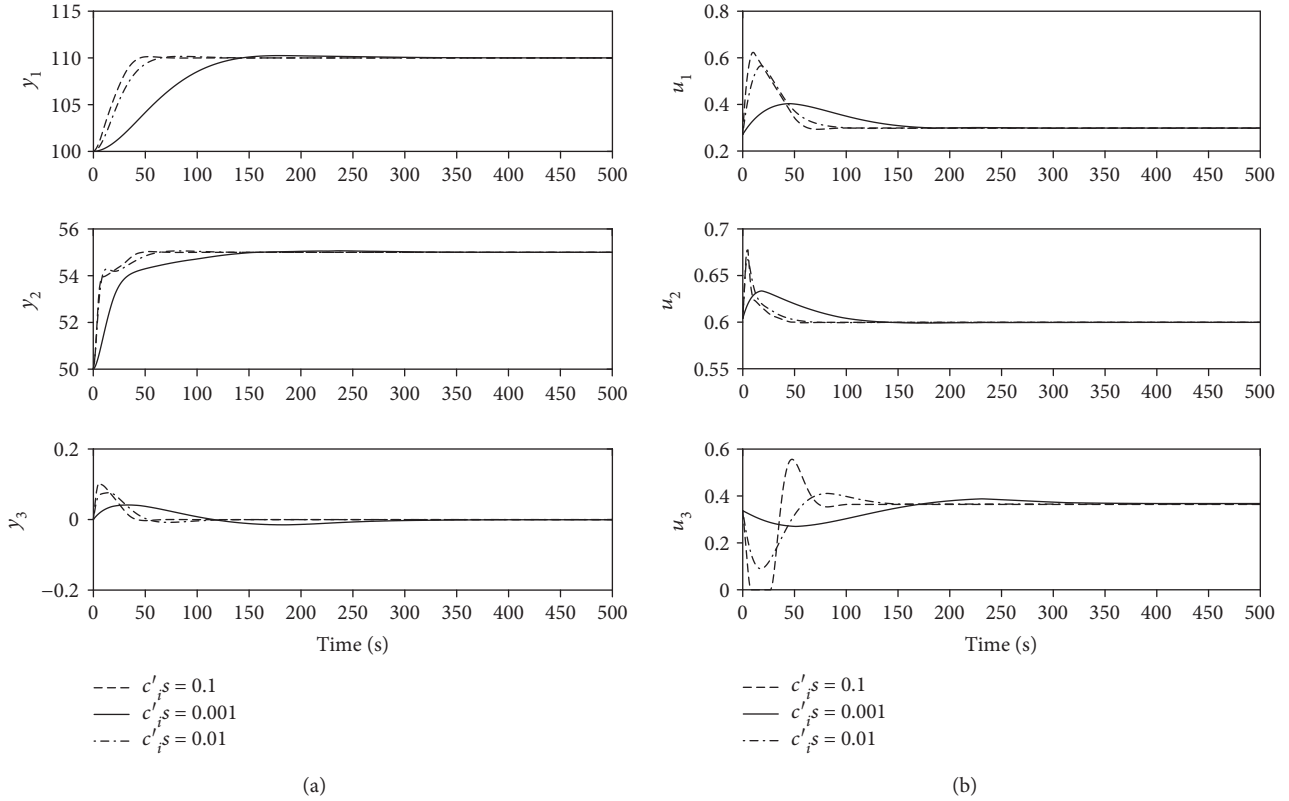


FIGURE 6: Outputs and controls of the unit when taking different values of expansion coefficients $c'_i s$.

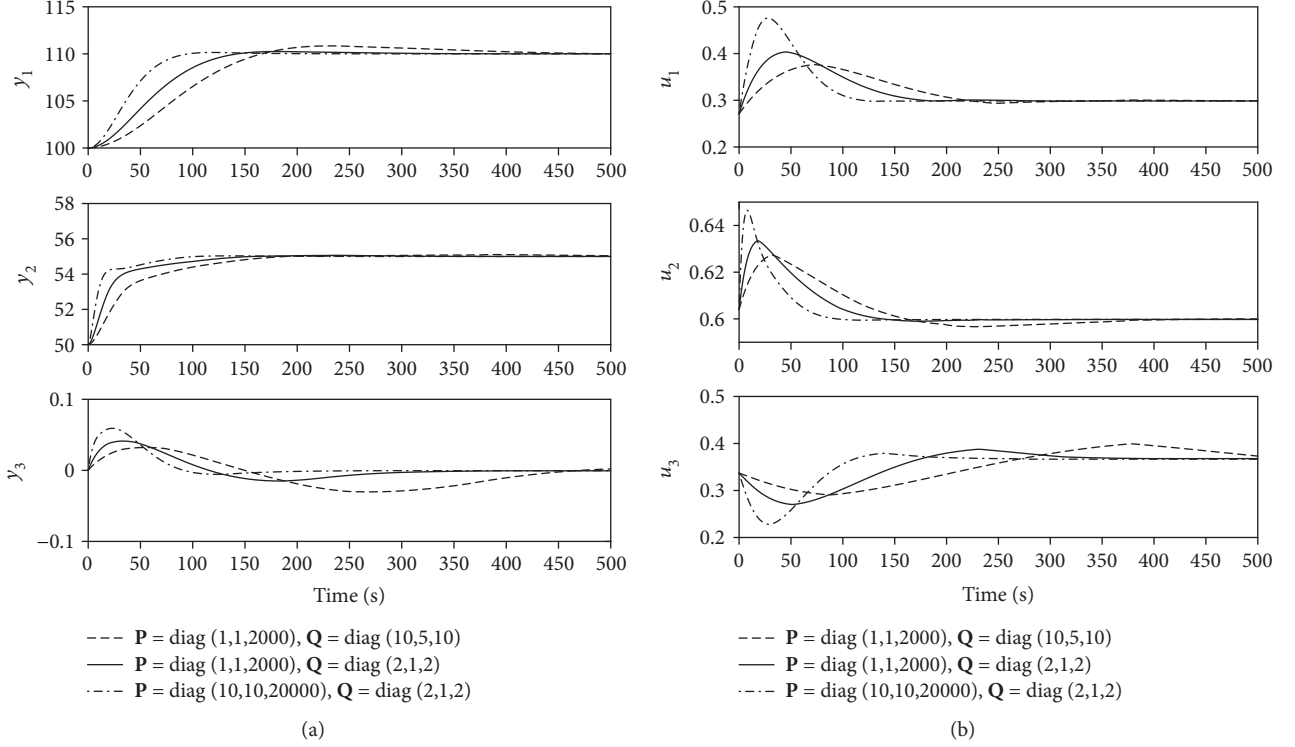


FIGURE 7: Outputs and controls of the unit when taking different values of \mathbf{P} and \mathbf{Q} .

$\mathbf{P} = \text{diag}\{10,10,20000\}$, $\mathbf{Q} = \text{diag}\{2,1,2\}$, and (3) $\mathbf{P} = \text{diag}\{1,1,2000\}$, $\mathbf{Q} = \text{diag}\{10,5,10\}$.

The results are shown in Figure 7. It can be seen from Figure 7 that the responses of the unit will arrive at their static setpoints faster by increasing \mathbf{P} or relatively decreasing \mathbf{Q} and that smaller control laws can be achieved when taking a larger value of \mathbf{Q} . One can select appropriate \mathbf{P} and \mathbf{Q} by considering the trade-off between the constraints on the output and control inputs.

From above discussions, we select the controller parameters as $\mathbf{P} = \text{diag}\{1, 1, 2000\}$, $\mathbf{Q} = \text{diag}\{2, 1, 2\}$, $N = 20$, and $c_i' s = 0.001$ for the consequent performance validations in what follows.

4.2. Performance Validation. This subsection presents the following three different study cases so as to further validate the performance of the receding Galerkin optimal controller.

Case 1. Receding Galerkin optimal control versus PID.

In this case, we compare the performances of receding Galerkin optimal control strategy and PID. We aim to drive the outputs to $y_r = [110, 55, 0]'$ from initial condition $x(0) = [100, 50, 449.5]'$, $y_3(0) = 0$, $\hat{x}_3(0) = 445$, and $u(0) = [0.271, 0.604, 0.337]'$. The 2-freedom PID controller saturated in bound $[0, 1]$ is designed as

$$\begin{aligned}
 u_{PID}(s) = & k_p(k_b y_r(s) - y(s)) + \frac{k_i}{s}(y_r(s) - y(s)) \\
 & + k_d \frac{k_N}{1 + (k_N/s)}(k_c y_r(s) - y(s)),
 \end{aligned} \quad (37)$$

with the following parameters

$$\begin{aligned}
 k_p &= [0.7646, 0.0118, 21.0424]', \\
 k_i &= [0.0455, 0.0023, 9.437]', \\
 k_d &= [-0.6708, -0.0005, -58.22]', \\
 k_b &= [0.8722, 0.0088, 0.3667]', \\
 k_c &= [01.68, 0.0088, 0.3667]', \\
 k_n &= [0.5917, 22.415, 0.3119]'.
 \end{aligned} \quad (38)$$

The results are shown in Figures 8, which demonstrates that the receding Galerkin method outperforms the 2-freedom PID controller. As can be seen from Figure 8, the outputs of the receding Galerkin method are much more smooth than that of PID and the control inputs' rate of change can be well guaranteed by the receding Galerkin method. Note that the receding Galerkin method can guarantee $y_3 \in [-0.1, 0.1]$, whereas the PID does not. Furthermore, it is difficult to guarantee the constraints imposed on the control inputs when applying PID.

Case 2. Wide-range load tracking.

In the second case, we intend to validate the tracking performance of the receding Galerkin method when the unit experiences in a wide-range load change. More precisely, we suggest here that the electrical output y_2 (MW) tries to track load demand 80 MW from a static condition 60 MW with a

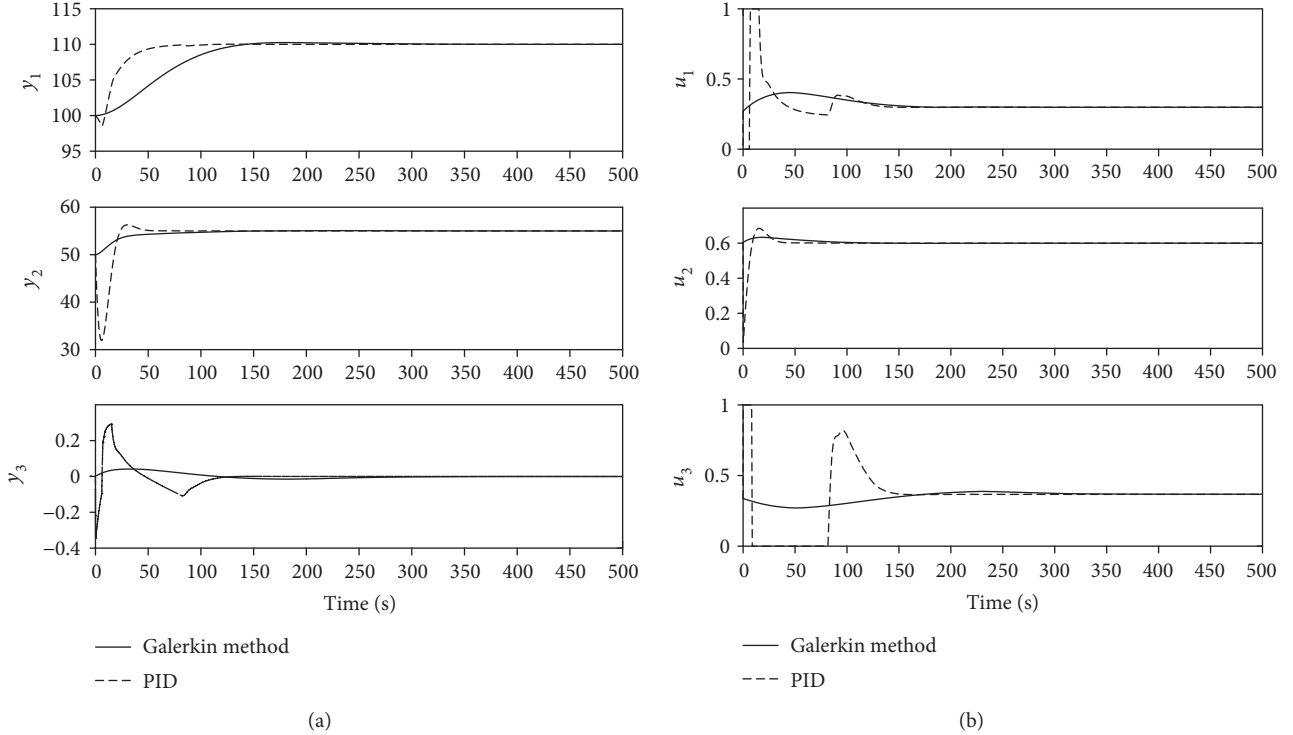


FIGURE 8: Outputs and controls of the unit by comparing with PID.

rate of 0.1 MW/s and then back to 50 MW with the same rate at time $t = 500$ s. Correspondingly, the drum steam pressure y_1 (kg/cm²) rises from 110 (kg/cm²) to 120 (kg/cm²) with a rate of 0.05 (kg/cm²/s) and descends back to 100 (kg/cm²) with a rate of 0.067 (kg/cm²). The drum water level y_3 has to vary in range $[-0.1, 0.1]$.

The simulation results are shown in Figure 9. It shows that the electrical output y_2 can track the load demands/references well and the drum water level y_3 satisfies output constraint $[-0.1, 0.1]$. As well, the drum steam pressure y_1 can also track the predefined reference well during the changes of load demands.

Case 3. Eliminating constant output disturbances using an independent model.

In the last case, we intend to show the performance of the receding Galerkin method with an independent model when constant disturbances exist in output channels. On the basis of Case 1, we suggest now that some constant disturbances appear in output channels at different times. More precisely, we define $d(t) = [d_1(t), d_2(t), d_3(t)]'$ such that

$$\begin{aligned} d(t) &= 0, & \text{if } t < 400, \\ d(t) &= [5, 5, 0.03]', & \text{if } 400 \leq t < 600, \\ d(t) &= [-5, -10, -0.05]', & \text{otherwise.} \end{aligned} \quad (39)$$

Figure 10 shows that the constant output disturbances d can be eliminated and the outputs of unit can track back to their original reference points. However, the control inputs

settle at their new steady points. It suggests that the independent model strategy is effective to estimate and thus eliminate the constant output disturbances.

Remark 5. From above simulations and discussions, we can see that optimal solutions can be really found by selecting appropriate tolerance δ^N and the order of approximation N , as already stated in Remark 4. The curves of the performance index are shown in Figure 11 in the cases of wide-range load tracking and existing constant output disturbances. We can see from Figure 11 that the performance indexes can finally converge to zero and then the unit arrived at static setpoints. This fact may suggest the stability of the closed-loop systems in an intuitive way.

Remark 6. The proposed receding Galerkin optimal control method can be in fact a general approach for a wide range of nonlinear systems rather than only for the boiler-turbine unit. For any nonlinear system, one just needs to design a state observer to estimate the unmeasurable states for this nonlinear system and then embed it into the receding Galerkin optimal controller, as that has been done for the boiler-turbine unit in this paper.

5. Conclusions

In summary, this paper proposes an adaptively receding Galerkin optimal control strategy for a nonlinear boiler-turbine unit. To deal with the problem of unmeasured state variable fluid density, a state observer is designed and

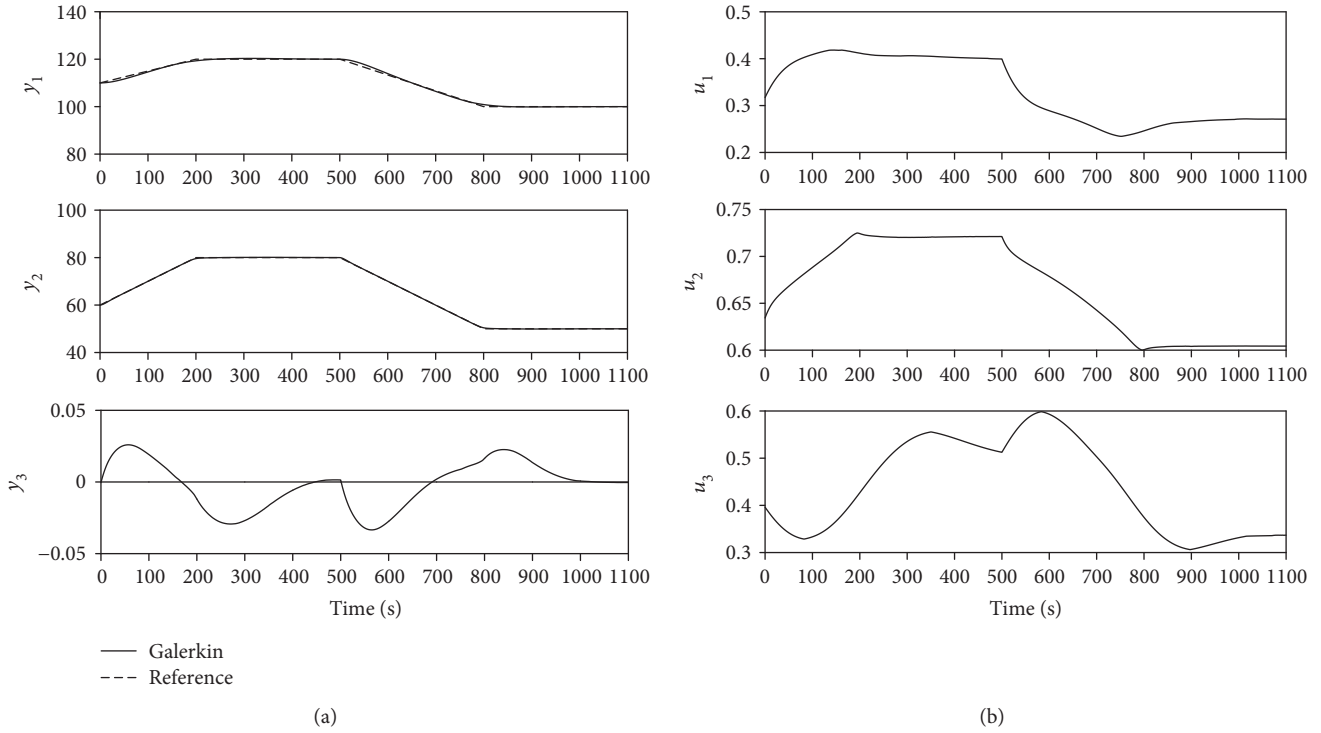


FIGURE 9: Outputs and controls of the unit in the case of tracking large-scale load reference.

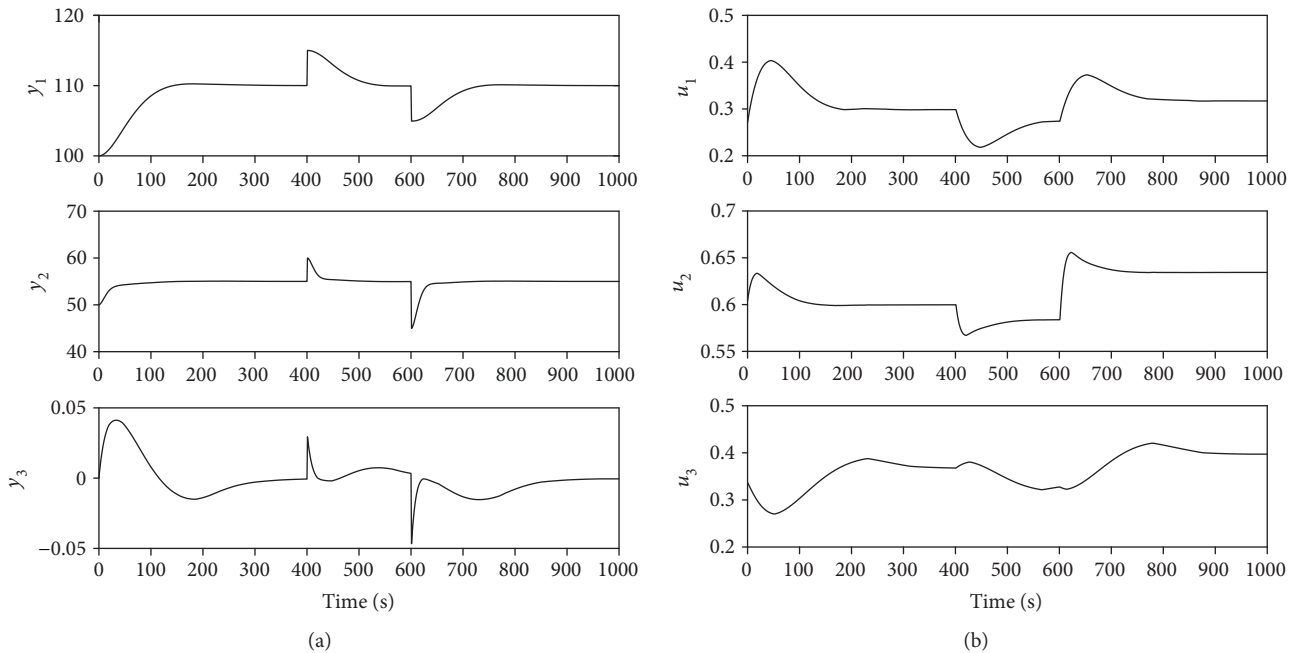


FIGURE 10: Outputs and controls of the unit in the case of existing constant output disturbances.

embedded into the receding Galerkin strategy. Meanwhile, an independent model structure is constructed in order to estimate and thus eliminate constant disturbances in output channels. Simulation results suggest that the unit can track load reference during wide-range operations

with satisfactory performance via this receding Galerkin optimal control strategy.

There are still some further interests. One most possible interest is to extend the proposed method to deal with lumped disturbances.

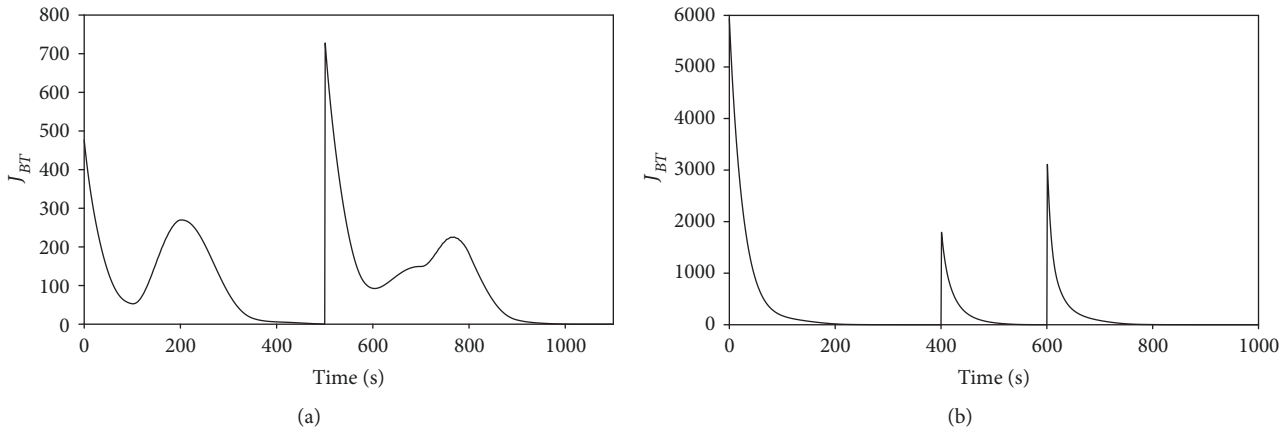


FIGURE 11: Performance indexes in the case of (a) wide-range load tracking and (b) existing constant output disturbances.

Data Availability

All the data are available in our article, and the readers who are interested in these data can contact the authors.

Conflicts of Interest

The authors declare that there are no conflicts of interest regarding the publication of this article.

Acknowledgments

This work is supported by Natural Science Foundation of China (51676034 and 51706093) and in part by the Key Project of Yunnan Power Grid Co. Ltd. (YNYJ2016043).

References

- [1] R. D. Bell and K. J. Astrom, "Dynamic models for boiler-turbine-alternator units: data logs and parameter estimation for a 160 MW unit," Technical report, Report tert-3192, Lund Institute of Technology, Sweden, 1987.
- [2] S. Zhang, C. W. Taft, J. Bentsman, A. Hussey, and B. Petrus, "Simultaneous gains tuning in boiler/turbine PID-based controller clusters using iterative feedback tuning methodology," *ISA Transactions*, vol. 51, no. 5, pp. 609–621, 2012.
- [3] S. Yang, C. Qian, and H. Du, "A genuine nonlinear approach for controller design of a boiler-turbine system," *ISA Transactions*, vol. 51, no. 3, pp. 446–453, 2012.
- [4] P.-C. Chen, "Multi-objective control of nonlinear boiler-turbine dynamics with actuator magnitude and rate constraints," *ISA Transactions*, vol. 52, no. 1, pp. 115–128, 2013.
- [5] P.-C. Chen and J. S. Shamma, "Gain-scheduled ℓ^1 -optimal control for boiler-turbine dynamics with actuator saturation," *Journal of Process Control*, vol. 14, no. 3, pp. 263–277, 2004.
- [6] F. Fang and L. Wei, "Backstepping-based nonlinear adaptive control for coal-fired utility boiler-turbine units," *Applied Energy*, vol. 88, no. 3, pp. 814–824, 2011.
- [7] S. Ghabraei, H. Moradi, and G. Vossoughi, "Multivariable robust adaptive sliding mode control of an industrial boiler-turbine in the presence of modeling imprecisions and external disturbances: A comparison with type-I servo controller," *ISA Transactions*, vol. 58, pp. 398–408, 2015.
- [8] S. Godoy, G. Scaglia, S. Romoli, R. Suvire, and O. Ortiz, "Trajectory tracking of boiler-turbine," in *2014 IEEE Biennial Congress of Argentina (ARGENCON)*, pp. 159–164, Bariloche, Argentina, June 2014.
- [9] M. Keshavarz, Y. Barkhoordari, and M. R. Jahed-Motlagh, "Piecewise affine modeling and control of a boiler-turbine unit," *Applied Thermal Engineering*, vol. 30, no. 8-9, pp. 781–791, 2010.
- [10] X. Kong, X. Liu, and K. Y. Lee, "Nonlinear multivariable hierarchical model predictive control for boiler-turbine system," *Energy*, vol. 93, pp. 309–322, 2015.
- [11] M. Lawrynczuk, "Nonlinear predictive control of a boiler-turbine unit: a state-space approach with successive on-line model linearisation and quadratic optimisation," *ISA Transactions*, vol. 67, pp. 476–495, 2017.
- [12] Y. Li, J. Shen, K. Y. Lee, and X. Liu, "Offset-free fuzzy model predictive control of a boiler-turbine system based on genetic algorithm," *Simulation Modelling Practice and Theory*, vol. 26, pp. 77–95, 2012.
- [13] X. Liu and X. Kong, "Nonlinear fuzzy model predictive iterative learning control for drum-type boiler-turbine system," *Journal of Process Control*, vol. 23, no. 8, pp. 1023–1040, 2013.
- [14] U. C. Moon and K. Y. Lee, "A boiler-turbine system control using a fuzzy auto-regressive moving average (FARMA) model," *IEEE Transactions on Energy Conversion*, vol. 18, no. 1, pp. 142–148, 2003.
- [15] X. Wu, J. Shen, Y. Li, and K. Y. Lee, "Data-driven modeling and predictive control for boiler-turbine unit," *IEEE Transactions on Energy Conversion*, vol. 28, no. 3, pp. 470–481, 2013.
- [16] X. Wu, J. Shen, Y. G. Li, and K. Y. Lee, "Data-driven modeling and predictive control for boiler-turbine unit using fuzzy clustering and subspace methods," *ISA Transactions*, vol. 53, no. 3, pp. 699–708, 2014.
- [17] S. Yang and C. Qian, "Controller design for a nonlinear drum-boiler turbine system," in *18th Annual Joint ISA POWID/EPRI Controls and Instrumentation Conference*, Scottsdale, AZ, USA, June 2008.
- [18] S. Yang and C. Qian, "Real-time optimal control of a boiler-turbine system using pseudospectral methods," in *19th Annual Joint ISA POWID/EPRI Controls and Instrumentation Conference and 52nd ISA POWID Symposium*, pp. 166–177, Rosemont, Illinois, USA, May 2009.

- [19] D. Yu and Z. Xu, "Nonlinear coordinated control of drum boiler power unit based on feedback linearization," *IEEE Transactions on Energy Conversion*, vol. 20, no. 1, pp. 204–210, 2005.
- [20] R. Sun, Q. Hong, and G. Zhu, "A novel optimal control method for impulsive-correction projectile based on particle swarm optimization," *Discrete Dynamics in Nature and Society*, vol. 2016, Article ID 5098784, 9 pages, 2016.
- [21] Q. Gong, W. Kang, and I. M. Ross, "A pseudospectral method for the optimal control of constrained feedback linearizable systems," *IEEE Transactions on Automatic Control*, vol. 51, no. 7, pp. 1115–1129, 2006.
- [22] R. Boucher, W. Kang, and Q. Gong, "Galerkin optimal control for constrained nonlinear problems," in *2014 American Control Conference*, pp. 2432–2437, Portland, OR, USA, June 2014.
- [23] R. Boucher, W. Kang, and Q. Gong, "Galerkin optimal control," *Journal of Optimization Theory and Applications*, vol. 169, no. 3, pp. 825–847, 2016.
- [24] G. Elnagar, M. A. Kazemi, and M. Razzaghi, "The pseudospectral legendre method for discretizing optimal control problems," *IEEE Transactions on Automatic Control*, vol. 40, no. 10, pp. 1793–1796, 1995.
- [25] J. Na, Q. Chen, X. Ren, and Y. Guo, "Adaptive prescribed performance motion control of servo mechanisms with friction compensation," *IEEE Transactions on Industrial Electronics*, vol. 61, no. 1, pp. 486–494, 2014.
- [26] S. Wang, X. Ren, J. Na, and T. Zeng, "Extended-state-observer-based funnel control for nonlinear servomechanisms with prescribed tracking performance," *IEEE Transactions on Automation Science and Engineering*, vol. 14, no. 1, pp. 98–108, 2017.
- [27] J. Yang, W. Zheng, S. Li, B. Wu, and M. Cheng, "Design of prediction-accuracy-enhanced continuous-time MPC for disturbed systems via a disturbance observer," *IEEE Transactions on Industrial Electronics*, vol. 62, no. 9, pp. 5807–5816, 2015.



Hindawi

Submit your manuscripts at
www.hindawi.com

